6

Weldability of Iron Based Powder Metal Alloys Using Pulsed GTAW Process

Edmilson Otoni Correa
Universidade Federal de Itajuba
Brazil

1. Introduction

In the last decades, powder metal (PM) iron-based alloys have been extensively used as structural parts in mechanical components due to their good balance between ductility and tensile strength, low cost, high performance, flexibility of manufacturing, good magnetic properties and corrosion resistance. Consequently, such PM components have emerged as an effective alternative for replacing machined parts, castings and forgings in many engineering applications. However, continued efforts are demanded for obtaining optimum combination of properties to withstand various service conditions.

When replacing forged, cast or machined parts, weldability is one of the important requisites expected of P/M parts in actual service conditions like in structural and automobile applications. This is due to the fact of many of these parts occasionally need to be joined to one similar part or dissimilar material as integrated components. The welding of dissimilar metal is generally more challenging than that of similar metals because of considerably difference in the physical, thermal, electrical, mechanical and metallurgical properties of the parts to be joined. In order to take full advantage of the dissimilar metals involved, it is necessary to produce high quality joints between them.

The welding of powder metal parts is different from welding of cast, rolled and forged parts due to the presence of porosities in their microstructure. The nature of the porosity is controlled by several processing variables such as green density, sintering, etc. In particular, the fraction, size, distribution and morphology of the porosity have a profound impact on mechanical behaviour, especially in components under welding conditions.

Fusion welding methods have been successfully used to join powder metal parts and are more related to the welding of medium and high density powder metal parts. Welding process such as gas tungsten arc welding (GTAW) and gas metal arc welding (GMAW) have been often cited as feasible possibilities to join PM structural parts. However, very little experimental information about welding parameters used, more adequate filler metal, etc., is available on the application of these welding process to join PM components.

This chapter will present a review of the main characteristics of the PM parts which differs them of the materials fully dense materials as it pertains to joining and the weldability of powder metal iron alloys using the pulsed gas tungsten welding process with filler metal.

2. Benefits of the powder metallurgy

The variety of materials, complexity of components and advances in manufacturing process make powder metallurgy (PM) an established process for the production of structural parts in mechanical components.

In conventional PM process (German, 2005; Jenkins & Wood, 1997; Lenel, 1980; Thummler & Oberacker, 1993; Schatt & Wieters, 1997) the part is made by four basic production steps including mixing elemental or alloy powder, compacting, debinding and sintering. The compacting step may be subdivided into three steps, namely powder filling, powder compacting and green compact rejecting. Normal concerns for powder filling are powder particle flow, filling height, powder particle packing and powder particle segregation.

During the compacting step, some phenomena including particle deformation, cold welding at points of contact and interlocking between particles occur. Concerns for powder compacting are friction between powder particles and between powder particles and die walls and density distribution of the compact. According to author (Middle, 1981), due to these friction effects during the compacting, the density distribution of the PM part after sintering may be very uneven and may produce a irregular shrink and, consequently, the nucleation and propagation of cracks in the thermal affected zone of the material subjected to fusion welding.

During the rejecting the compact from the die (spring back), the compact volume expansion to release stored residual stress is the most important factor. If the spring back occurs too fast with high magnitude, it will cause undesirable deterioration of the compact.

Debinding and sintering, in general, are carried out in the same furnace. Parameters that influence both processes, including temperature, time and furnace atmosphere have to be optimized. The optimum conditions for debinding and sintering of a certain type powder metal part in the specified furnace are important for obtaining a good metallurgical bond between the powder particles and, consequently, a PM part with good mechanical resistance (German, 2005; Jenkins & Wood, 1997; Lenel, 1980; Thummler & Oberacker, 1993; Schatt & Wieters, 1997).

The PM process typically uses more than 95% of the starting raw material in the finished part and only minor machining is required. Because of this, PM process is an energy and material conserving process as well as cost effective in producing simple or complex parts at very close final dimensions in production rates which can range from a few hundred to several thousand parts per hour. PM process also may be sized for closer dimensional control for both, higher density or strength (Metal Powder Industry Federation [MPIF], 2004).

The versatility of PM is applied in numerous industries, including automotive, aerospace, electrical and electronic equipments, agricultural equipments and power tools. PM parts design serve these industries in a wide range of engineering applications which fall into two main groups: In one group are parts of difficult-to-fabricate materials by other manufacturing process such as tungsten and molybdenum, porous bearing, magnetic parts, etc. Another group consists of PM ferrous components increasingly attractive in replace machined parts, castings and forgings. In this group there are more material systems and requires to meet the requirements of more demanding applications.

The benefits of the PM process may be summarized as follows:

- Eliminates or minimizes the machining
- Eliminates or minimizes scrap losses

- Maintain close dimensional tolerances
- Permits a wide variety of alloy systems
- Produces good surface finishes
- Provides materials which may be heat-treated for increased strength or increased wear resistance
- Facilitates manufacture of complex or unique shapes which would be impractical or impossible with other metalworking processes.
- Suited to moderate-to high volume component production requirements
- Offers long-term performance reliability in critical applications
- Cost effective
- Provides controlled porosity for self-lubrification or filtration

3. Weldability of ferrous PM materials

3.1 Influence of the porosity

The most prominent microstructural feature of a PM component is its porosity, which affects virtually all its physical properties and, consequently, its weldability. The nature of the porosity is controlled by several processing variables such as green density, sintering temperature and time, alloying additions, and particle size and type of the initial powders. In particular, the fraction, size, distribution and morphology of the porosity have a profound impact on mechanical behaviour, especially in components under welding conditions (Chawla & Deng, 2005; Sudhakar et al., 2000).

Firstly, the pores act as thermal insulators which slow the transfer of heat, affecting considerably the thermal conductivity of the PM material to be joined. As the change in heat transfer naturally affects the welding parameters, the welder needs constantly to adjust them to assure the good quality of the weldment. Also, since the amount of porosity reduces the thermal conductivity, the cooling rate of the material also slows, reducing the hardening tendency (Hamill, 1993; Kurt et al., 2004; Kumar et al., 2007).

The thermal expansion is another important physical characteristic which is influenced by the porosity. Potential changes in the porosity volume fraction during welding, due to smaller particle melting or filler metal infiltration, can result in excessive shrinkage or growth. As a consequence, subsequent cracking can occur in the heat affected zone (HAZ) or in the fusion zone (ZF) of the PM base metal.

Porosity can also cause erratic fluctuations in welding performance as well as other welding defects because of entrapped oxides or impurities within the structure. These oxides and impurities may be originated from lubricant residues and quench oils.

3.2 PM welding process

The selection of the welding process more suitable to join PM parts should be made taking an account the requirements desired such as strength, environmental factors, appearance and the porosity volume. According to the literature (Hamill, 1993; Jayabharat et al., 2007), fusion welding processes are used successfully to join ferrous powder metal parts with high density (> 7.0 g/cm^3) once these high density PM parts typically have the same weldability as forged, rolled or cast materials. Indeed, research of Hinrichs et al showed that it is possible to obtain good quality dissimilar weldments of low and medium carbon PM steels joined with forged steels using the most common fusion welding processes. The researchers

also showed that in the case of the welding of PM high-strength low-alloy (HSLA) steels, procedures such as pre-heating and hydrogen control should be adopted to guarantee the success of the joining.

Low and intermediate density PM parts (< 7.0 g/cm^3) should be joined using welding processes which minimize the volume of molten weld metal such as resistance projection welding, friction welding and brazing.

The reason is that the low fracture resistance of these PM materials, caused by the small number of bonding between the particles, does not allow that these absorb the residual stress produced by the high densification that occurs in the heat affected zone and shrinkage of the weld metal, resulting in subsequent cracking in or near the weld interface. Additionally, when choosing the brazing process to join the low or intermediate density PM parts, a special attention should be paid to the capillary force o f the pores once the porosity near the joint wicks the copper brazing filler metal into the pores, leaving an insufficient amount of filler metal to establish the satisfactory weld strength. To overcome this problem, the PM parts must be copper infiltrated before brazing (Hamill, 1993; Jayabharat et al., 2007).

4. Pulsed GTAW process

The Gas Tungsten Arc Welding (GTAW) is a fusion welding process, where arc is produced between non-consumable tungsten electrode and base metal. This process provides suitable results in many situations because of its ability to control the welding parameters (heat input, travel speed, feed rate and type of filler metal) during the welding and subsequent weld metal and HAZ hardness. The higher control of the heat input in this process compared with other fusion welding processes may be mainly attributed to the fact of the welding arc does not suffer direct interference of the metal transference during welding.

Pulsed GTAW involves cycling of the welding current from a high level to a low level at a selected regular frequency. Thus, pulsing the current introduces additional operational parameters, which include peak current, base current, peak pulse time and base pulse time (Pawan et al., 2011). Figure 1 shows the representation for the pulsed current.

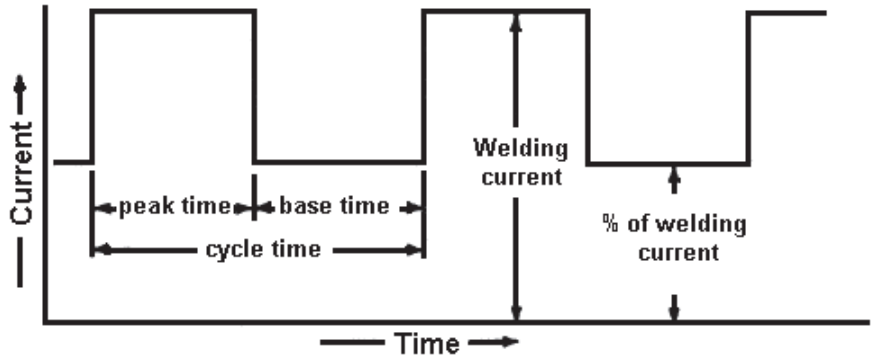

Fig. 1. Representation of the pulsed current.

Pulsed GTAW is frequently used for welding of several materials as heat input can be precisely controlled. Also, this process is strongly characterized by the bead geometry control, which plays an important role in determining the mechanical properties of the weldment (Juang & Tarng, 2002).
In contrast to continuous current welding, in the pulse mode the heat energy required to melt the base material is supplied only during peak current pulses for brief intervals of time allowing the heat to dissipate into the base material. With this, it is possible to achieve the maximum penetration without excessive heat build-up (Juang & Tarng, 2002).
As a result of all mentioned above, it is possible to obtain weldments with a narrower HAZ as well as reduction of segregation of alloying elements, of residual stress and of the hot cracking sensitivity (D' Oliveira et al., 2006; Wang et al., 2006). Current pulsing also results in periodic variations of the arc forces and in an increase of the melt pool agitation leading to additional fluid flow, which lowers the temperature in front of the solidifying interface. This temperature fluctuations leads to the continual changes in the weld pool size and shape favouring the growth of new grains (Pawan et al., 2011).
As a consequence of this grain refinement in the fusion zone, an improvement of the mechanical properties, such as tensile and fatigue resistance is achieved. Therefore, through the use of pulsed parameters, it is possible working with high current peaks without increase the average heat input to the base material, which enables itself as a good choice for welding powder metals alloys.

4.1 Weldability study of iron based powder metal alloys

According to the literature (Hamill, 1993), a unique conventional GTAW application involving welding of PM parts was the replacement of a casting for two welded PM components together for use in a commercial truck differential. It was found that the welded PM components exhibited higher and more consistent strength values than a bolted gray iron casting along with providing a 35% cost savings compared with the previous method of manufacture. However, there was not enough information about the welding procedures (parameters, heat input, gas shield flow, etc) used to carry out the welding.
This topic therefore intends to provide to the readers experimental information about welding of iron based PM alloys using the pulsed GTAW.
The materials involved in this study were three different iron based powder metal alloys whose compositions and features are given in table 1. As mentioned before, these alloys are the largest and the most effective alternative PM parts group for replacing castings, forged and machined parts, mainly in the automobile industry.

P/M alloys	Chemical composition (wt-%)			Raw material		
	Fe	Ni	P	Powder	Particle size range (μm)	Apparent density (g/cm^3)
Fe	100	-	-			
Fe-Ni	96.00	4.00	-	Sponge iron	60-150	2.8-3.1
				Carbonyl nickel	3	-
Fe-Ni-P	95.75	4.00	0.25	Pre-alloyed Fe-P (20wt-% P)	< 44	-

Table 1. Specification of the powder metal alloys.

In order to obtain the PM alloys, the powder metal were first mixed with lubrificant (zinc stearate) in a ball mill according to the chemical compositions of the alloys given in table 1 to produce a homogeneous mixture of ingredients. After that, the mixed powder of each alloy was compacted to about 90% relative density in a press (green compact) and then sintered in a pure hydrogen atmosphere according to the thermal cycle shown in Figure 2 to complete the metallurgical bonds between powder particles.

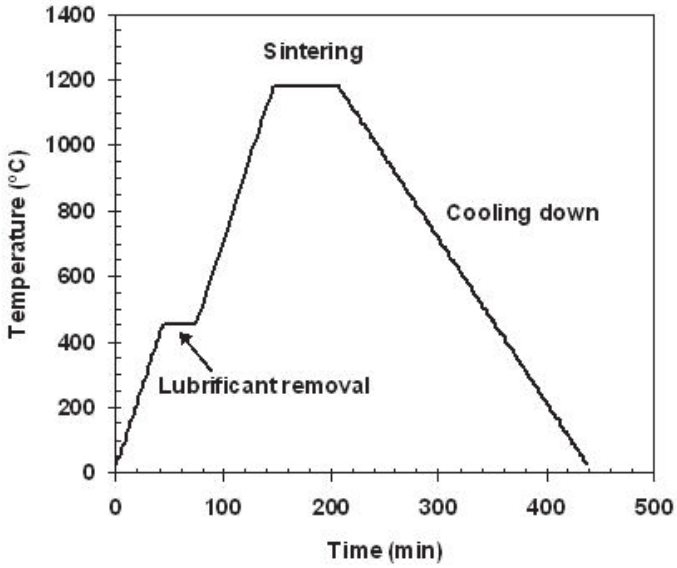

Fig. 2. Thermal cycle of sintering.

The powder metal samples (dimensions: 100 mm x 20mm x 7 mm) produced were welded in the butt joint, flat position with three different filler metals (AWS R 70s-6, AWS R 309L, AWS R Fe-Ni) using four passes weld by a manual pulsed GTAW process. The pulse welding parameters used were the same to the three different alloys and were chosen after preliminary tests that guaranteed an arc stability and lower heat input. A flow rate of argon (99.99% purity) of 7 l/min was used as a shielding gas. The travel speed was adjusted to give an adequate penetration and weld bead contour. These welding parameters are given in table 2.

	Parameters				
	Peak current (I_p)	Base current (I_B)	Peak time (T_P)	Base time (T_B)	Filler metal
Alloy	(Amps)	(Amps)	(s)	(s)	
Fe	140	80	0.40	0.40	AWS R 70S-6 (Ø 1,6 mm)
Fe-Ni	140	80	0.40	0.40	AWS R 70S-6 (Ø 1,6 mm)
Fe-Ni	140	80	0.40	0.40	AWS R FeNi (Ø 3,25 mm)
Fe-Ni-P	140	80	0.40	0.40	AWS R FeNi (Ø 3,25 mm)
Fe-Ni-P	140	80	0.40	0.40	AWS R 309L (Ø 2,4 mm)

as: Argon, Shielding gas flow rate: 7 l/min, DCEN polarity, Backing shielding gas flow rate: 10 l/min

Table 2. Pulsed GTAW parameters.

After welding, the test samples were transverse sectioned, polished with Al_2O_3 and etched with 2% nital (HNO_3 + alcohol). Microstructural examination of the specimens was carried out using standard optical microscopy and scanning electronic microscopy (SEM). Vickers hardness values were taken across the transverse section using a 10 Kg load. The tensile test samples geometry is shown in Figure 3 and these were in accordance with ISO 2740 standard.

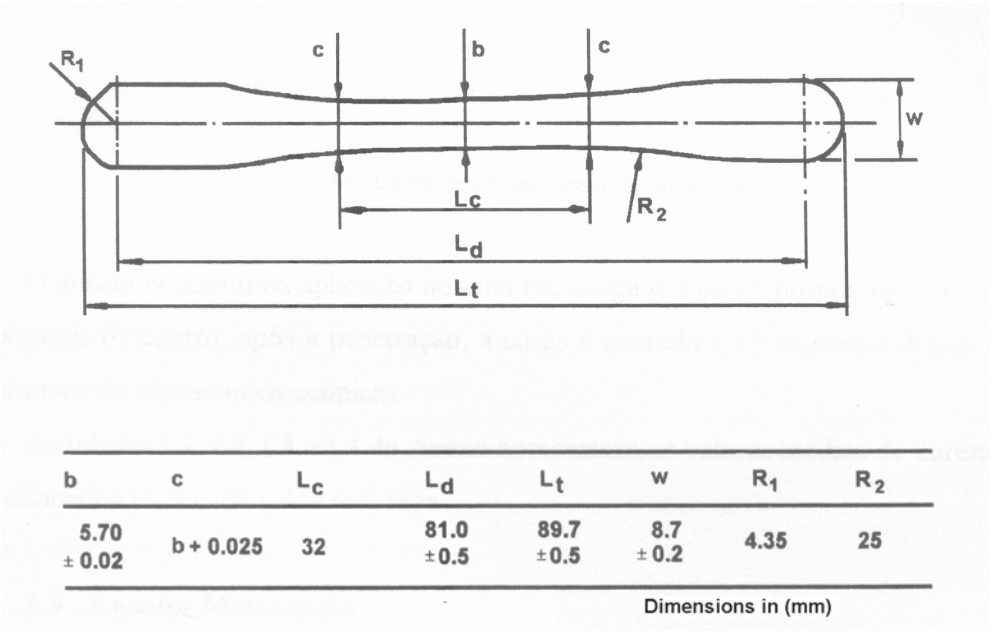

b	c	L_c	L_d	L_t	w	R_1	R_2
5.70 ± 0.02	b + 0.025	32	81.0 ±0.5	89.7 ±0.5	8.7 ± 0.2	4.35	25

Dimensions in (mm)

Fig. 3. Tensile test samples geometry.

4.1.1 Microstructural characterization of the weldments

a. Powder metal pure Fe and Fe-Ni alloy

As shown in Figures 4, 5 and 6, no difficulty concerning to the weldability of 7-mm thickness samples of powder metal pure Fe using filler metal of mild steel and Fe-Ni alloy using filler metal of mild steel and Fe-Ni alloy (60% Fe-40% Ni) was observed. Metallographic examinations showed the presence of small pores in the base metal of the alloys randomly distributed in a ferritic matrix. Meanwhile, no porosity and shrinkage cracks were observed in the weld metal and heat affected zone of the weldments. This may be mainly attributed to the high density after sintering (> 7.0 g/cm^3) and, in lesser extension, to the small size of the pores.

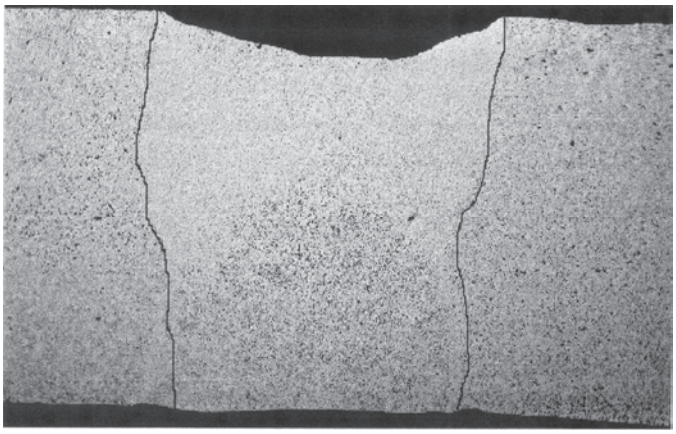

Fig. 4. Macrograph of weld of 7 mm powder metal pure Fe using filler metal of mild steel. The black lines outline the fusion zone. Etching: 2% nital. Magnification: 15x.

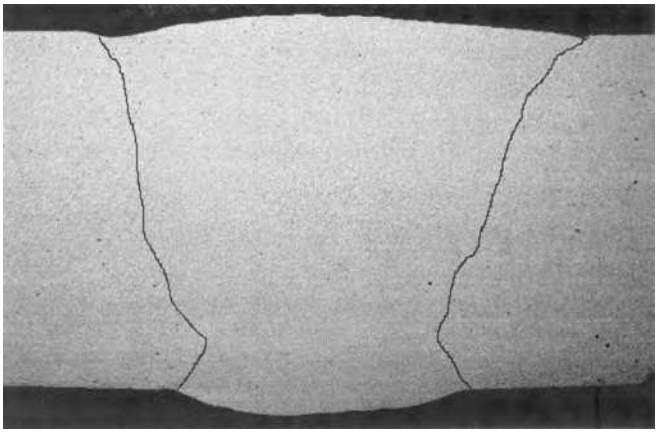

Fig. 5. Macrograph of weld of 7 mm powder metal Fe-Ni alloy using filler metal of mild steel. The black lines outline the fusion zone. Note the good mixing between the filler metal and base metal. Etching: 2% nital. Magnification: 15x.

Fig. 6. Macrograph of weld of 7 mm powder metal Fe-Ni alloy using filler metal of Fe-Ni alloy (60%Fe-40% Ni). Etching: 2% nital. Magnification: 15x.

Figures 7, 8 and 9 showed that the powder metal pure Fe and Fe-Ni alloy did not evidence significant changes of hardness profile in the HAZ in comparison with base metal for the filler metals used in this study, which is an indicative of a good continuity of mechanical properties after welding.

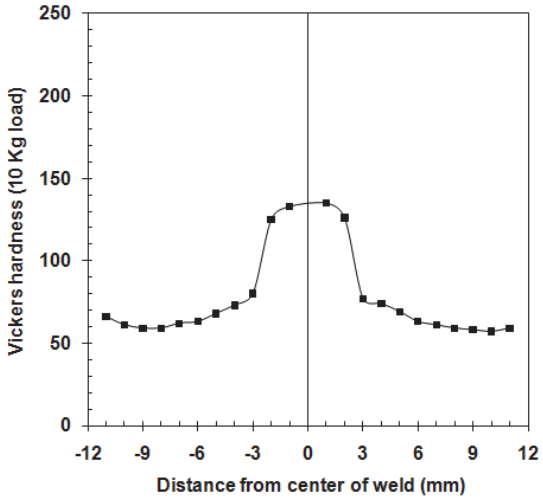

Fig. 7. Hardness profile through the powder metal pure Fe using filler metal of mild steel.

In general, phosphorus is intentionally added in powder metal iron based alloys to increase the densification of the iron powder once this element allows the formation of a transient liquid phase during sintering. Furthermore, phosphorus is known to improve the corrosion resistance and magnetic properties of the powder metal iron-based parts (ASM Handbook,

1999). However, phosphorus additions are not particularly attractive for fusion welding applications because its presence in the metal base composition is associated with the formation of the eutectic M_3P, which may promote solidification cracking in the fusion zone. Therefore, the amount of phosphorus added in the alloy must be rigorously controlled (Correa et al., 2008).

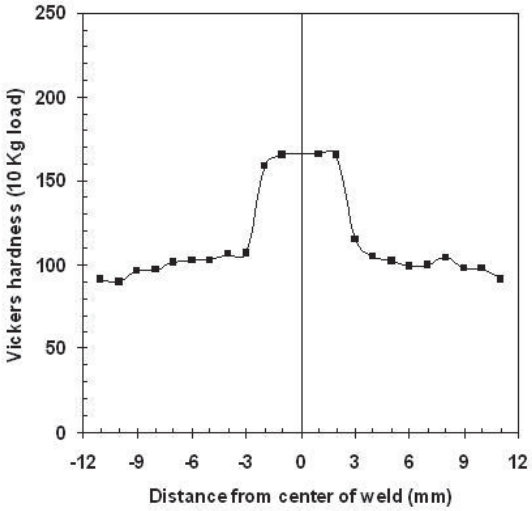

Fig. 8. Hardness profile through the powder metal Fe-Ni alloy using filler metal of mild steel.

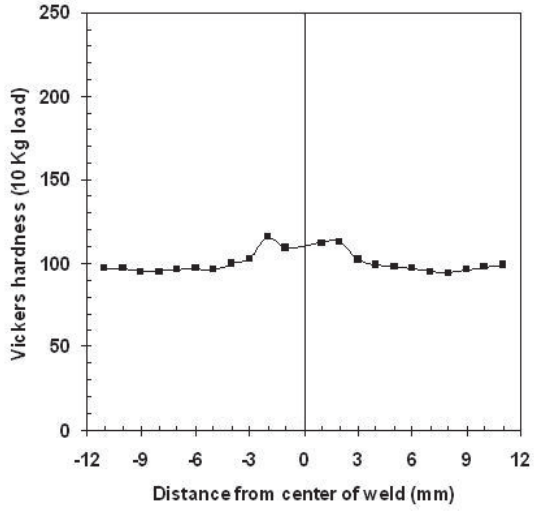

Fig. 9. Hardness profile through the powder metal Fe-Ni alloy using filler metal of Fe-Ni.

b. Powder metal Fe-Ni-P

According to author (Beiss, 1989), PM carbon steels with additions of 0,35% P may be fusion successfully welded without the occurrence of solidification cracks since the carbon content is lower than 0,2%. PM carbon steels with higher carbon contents tend to facilitate the segregation of the phosphorus and the formation of the M_3P eutectic.

Figure 6 shows the microstructure of the transverse section of weld joint of the alloy Fe-Ni-P using Fe-Ni (60% Fe-40% Ni) filler metal. Despite the good toughness of the Fe-Ni filler metal to absorb the shrink stresses during the weld metal cooling, the weld metal presented solidification cracks and pores after the pulsed GTA welding.

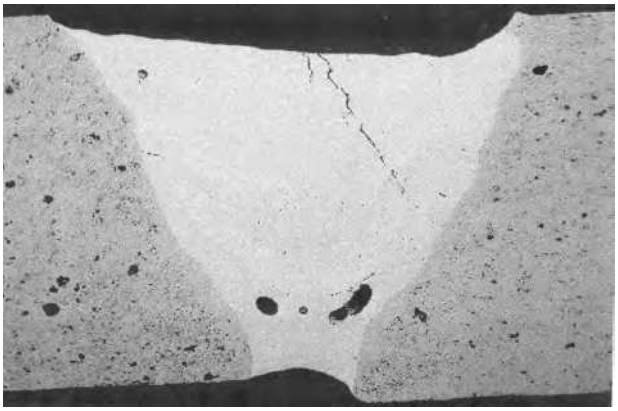

Fig. 10. Macrograph of weld of 7 mm powder metal Fe-Ni-P alloy using filler metal of Fe-Ni (60% Fe-40% Ni). Note the presence of solidification cracks and porosity in the fusion zone. Etching 2%. Magnification: 15x.

The weld solidification cracking can be mainly attributed to the presence of the low-melting eutectic Fe_3P and/or Ni_3P in the weld pool. According to the literature (Lancaster, 1987; Lippold & Kotecki, 2005), the excessive amount of phosphorus combines with nickel or iron forming the low-melting eutectic Ni_3P or Fe_3P. The continuous presence of the segregated Ni_3P or Fe_3P liquid film in the last stages of solidification o fthe weld pool combined with the higher shrinking stress due to faster cooling rates during fusion welding, may have contributed to the appearance of solidification cracking (Briskman, 1979). In addition, considering the potential of the nickel as an austenite stabilizer, the Fe-Ni filler metal solidifies in the austenitic mode, which increases the segregation of phosphorus in the weld pool and, consequently, the susceptibility to cracking (Lippold & Kotecki, 2005).

Figures 11 and 12 show the presence of phosphorus eutectic in the HAZ and fusion zone of the powder metal Fe-Ni-P alloy using Fe-Ni filler metal, which is characterized by the presence of small "islands" in the ferritic grains.

As can be seen in Figure 13, a complete elimination of the weld solidification cracking and porosity in the fusion zone of the Fe-Ni-P alloy was possible using the filler metal 309L stainless steel and adjusting the welding parameters to those values shown in table 2. According the literature (Lippold & Kotecki, 2005), the principal reason for the absence of solidification cracking in the weld metal of the 309L filler metal is the low carbon content of the 309L filler metal and, mainly, the presence of a two-phase austenite/ferrite mixture in the microstructure of the weld metal.(See Fig 14).

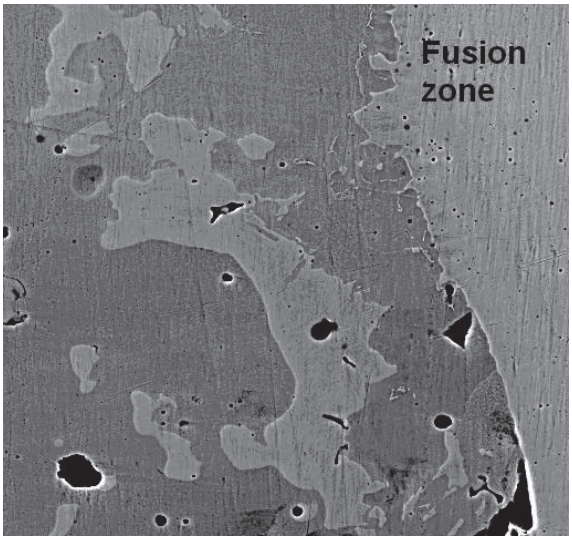

Fig. 11. Micrograph of the HAZ of the powder metal Fe-Ni-P alloy. Note the presence of the phosphorus eutectic islands in the ferritic grains and some pores. Etching: 2% nital. Magnification 800x.

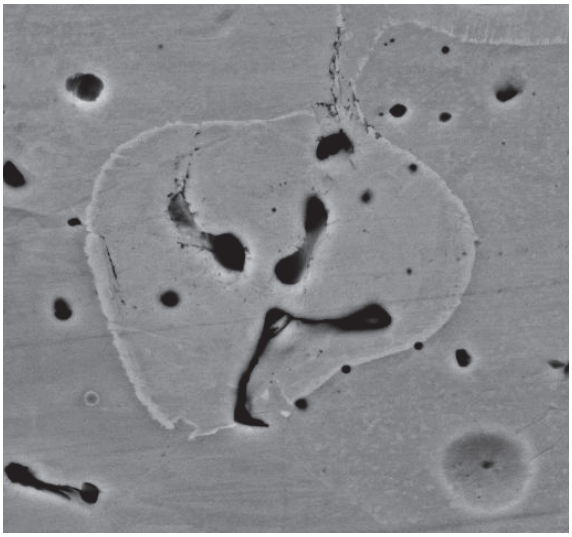

Fig. 12. Micrograph of the fusion zone of the powder metal Fe-Ni-P alloy. Note the presence of the phosphorus eutectic in the ferritic grains and some pores. Etching: 2% nital. Magnification: 2000x.

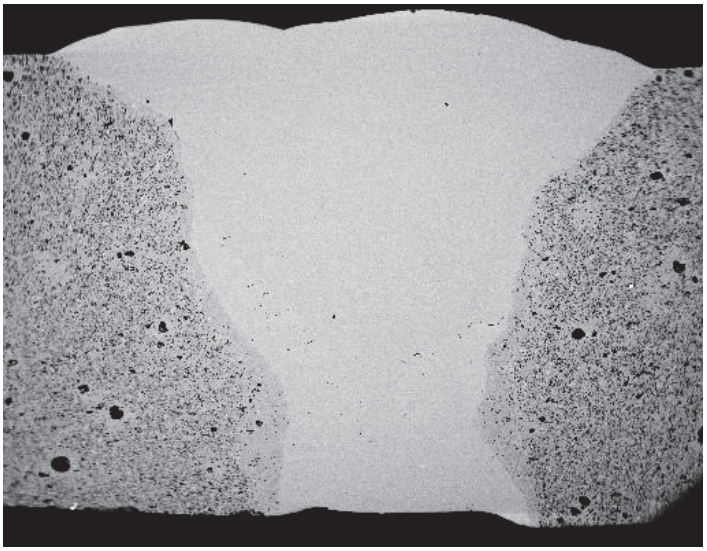

Fig. 13. Macrograph of weld of 7 mm powder metal Fe-Ni-P alloy using filler metal of 309L stainless steel. Note the absence of solidification cracks and pores in the fusion zone. Note also large pores in the base metal. Etching: nital 2%. Magnification: 15x.

Fig. 14. Micrograph showing the two-phase austenite + vermicular delta ferrite mixture in the weld metal of 309L stainless steel. Etching: (HCl/HNO_3) reagent. Magnification: 1600x.

Image analysis results (Table 3) from optical micrographs, similar to that showed in Fig 14, together with observations in the WRC-1992 diagram, indicated that the ferrite number (FN) in the 309L stainless steel weld metal was approximately 7 FN. In general, above 3 FN, but less than 20 FN, solidification of austenitc stainless steels is most likely in the FA mode (Suutala, 1983).

309L stainless steel weld metal		
Statistical function	Phase A (Delta ferrite)	Phase B (Austenite)
Unity	%	%
Counts	15	15
Mean	6,77	93,23
Standard deviation	0.89	2.82

Table 3. Image analysis results of the delta ferrite volume fraction of the 309L weld metal.

In the FA mode, the duplex microstructure (delta ferrite + austenite) presents at the end of solidification, increase the amount of tortuous phase boundaries that resist wetting by liquid films and along which cracks might propagate. Thus, once the crack is nucleated, it becomes very difficult for it to propagate along to the nonplanar crack path generated to these tortuous bondaries (Briskman, 1979). Additionaly, as the solubility of the phosphorus in the ferrite is higher than that observed in the austenite, the delta ferrite in the weld metal is prone to absorb a significant amount of this element, which reduce the concentration of the phosphorus in liquid film, avoiding the permanence of the segragated low-melting eutectic until the last stages of solidification and, consequently, the solidification cracking.
It can be also seen in Fig. 14 the vermicular morphology of the delta ferrite. In general, this ferrite morphology is present when welding cooling is moderate and/or when the Creq/Nieq is low but still within the FA mode (Lippold & Kotecki, 2005).
It is worthwhile mentioning that other significant factors involving the pulsed GTA welding of teh powder metal Fe-Ni-P alloy may have also contributed to minimize the occurence of solidification cracking. These may be, for instance the utilization of pulsed current and multipass weld, which have the effect of refinement of the as-cast microstructure in the fusion zone (Balasubramanian et al., 2008).
Also, it can be noted that there was no presence of pores in the weld metal. However, th e pores in the base metal of this alloy (see Fig. 15) were large and rounded with higher densification of ferrite in their surroundings. The size of the Fe-P pre-alloyed particles added in this alloy probably is the cause of the pores characteristics (large and rounded) in the base metal.
Figure 16 shows that Fe-Ni-P alloy welded with 309L austenitic stainless steel filler metal did not evidence significant changes of hardness profile in the HAZ in comparison with the base metal, even though the phosphorus is prone to harden the ferrite by solid solution.

4.1.2 Tensile tests of the weldments

Tensile tests carried out in the welded samples of the pure Fe and Fe-Ni using AWS R 70S-6 and AWS R Fe-Ni filler metals (filler metal of mild steel and Fe-Ni alloy) and Fe-Ni-P powder metal alloy using AWS R 309L filler metal showed that the failures of samples occurred always in the base metal. Furthermore, the welded samples of these alloys presented ultimate tensile strength slightly higher than unwelded samples (see Table 4).
The higher tensile strength of the welded samples may be attributed to the residual stress in the samples due to their small dimensions (width and length) combined with the high heat input and the relatively rapid cooling of the weld metal during welding. It is worthwhile

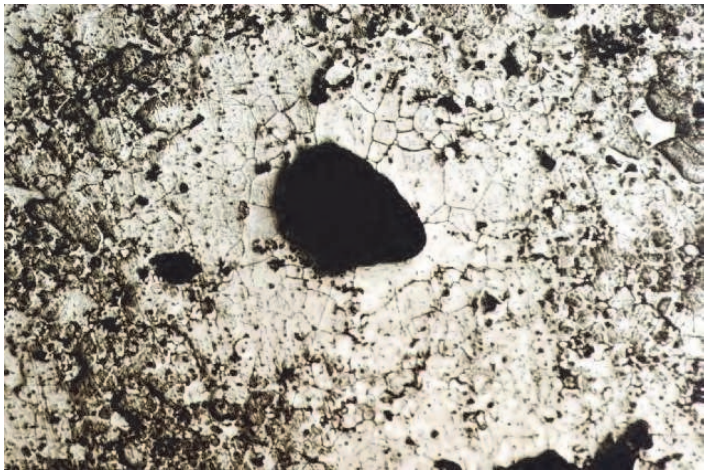

Fig. 15. Micrograph showing the large and rounded pore in the base metal. Note the high densification of ferrite in its surroundings . Etching: nital 2%. Magnification: 1600x.

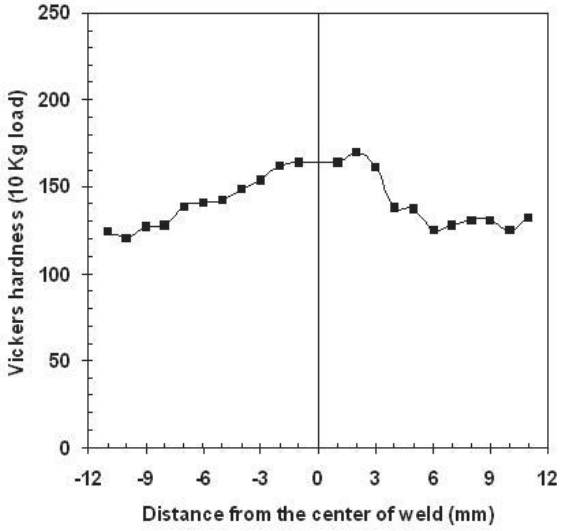

Fig. 16. Hardness profile through the powder metal Fe-Ni-P alloy using 309L stainless steel filler metal.

mentioning that the welded samples were not annealed after welding. However, the tensile tests results together with the hardness results indicated that weldments of these materials presented a good continuity of the mechanical properties with relation to the base metal, even when these materials are welded by a fusion welding process.

Tensile Properties	Unwelded samples			Welded samples		
	Fe	Fe-Ni	Fe-Ni-P	Fe	Fe-Ni	Fe-Ni-P
Ultimate tensile strength (MPa)	170	205	200	197	215	218
Elongation (in 25.4 mm) (%)	4.3	4.1	1.6	3.8	3.9	1.5

Table 4. Tensile properties of GTA welded alloys.

5. Conclusion

In this chapter was shown the benefits of the PM components and the advantages of their utilization in replacing casting, machined and forged materials. However, experimental information about joining these PM materials using fusion welding processes is still scarce.
Through of the study presented in this chapter, it was possible to verify that PM iron based alloys pure Fe and Fe-Ni may be successfully welded by pulsed GTAW process without additional techniques such as preheating, post-heating or special joint configuration.
Concerning to the Fe-Ni-P alloy, this alloy also may be successfully welded by pulsed GTAW process but a discerning selection of the filler metal and careful control over the welding parameters (heat input, peak current, base current, peak time, base time and travel speed) must be done. Due to the presence of phosphorus, the correct selection of the filler metal may avoid the presence of low-melting eutectic films at the end of the solidification and, consequently, the solidification cracking. A rigid control of the heat input, in turn, prevents the higher dilution of the base metal, which decreases the shrink stress in the fusion zone during the solidification of the weld pool leading to a lower susceptibility to cracking of the weldment.
Hardness results showed that no excessive hardening was observed in the weld metal and HAZ of the iron powder metal alloys studied. This is in agreement with the base metal fracture location in the tensile tests and with the slight increase of the tensile properties of welded samples in comparison with unwelded samples. In general, excessive hardening (higher Vickers hardness values) is prone to increase significantly the tensile strength and decrease the toughness.

6. Acknowledgment

The author acknowledges the Brazilian Government Agencies CNPq, CAPES and FAPEMIG for the financial support to carry out this study.

7. References

ASM Handbook, (1999). M*etallography and Microstructure,*, vol. 9, ASM, USA
Briskman, A.N. (1979). The effect of welding currente pulses on the susceptibility of weld metal to hot cracking during argon TIG welding, *Aut. Weld. (7)*, pp. 40-43.

Balasubramanian, M., Jayabalan, V. & Balasubramanian, V. (2008). Optimizing the Pulsed Current GTAW parameters to Attain Maximum Impact Toughness, M*aterials and Manufacturing Processes*, Vol. 23, n. 1-2, pp. 69-73.

Beiss, P. (1989). Finishing Process in Powder Metllurgy, *Powder Metallurgy*, 32 (4), pp. 277-284.

Chawla, N. & Deng, X. (2005). Microstructure and Mechanical behaviour of porous sintered steel, *Materials Science and Enginnering A, 390,* pp. 98-112.

Correa, E.O., Costa, S.C. & Santos, J.N. (2008). Weldability of iron based powder metal using pulsed plasma arc welding process, *Journal of Materials Processing Technology*, 198, pp. 323-329.

D' Oliveira, A.S.C.M., Paredes, R.S.C., & Santos, R.L.C. (2006). Pulsed Current Plasma Transferred Arc Hardfacing, *Journal of Materials Processing Technology,* 171, pp. 167-174.

German, R.M. (2005). Powder Metallurgy and Particulate Materials Processing, *Metal Powder Industries Federation*, New Jersey, USA.

Hamill, J.A. (1993). Pwhat are the joining process, Materials and Techniques for Powder Metal Parts, *Welding Journal*, 2, pp. 37-45, USA.

Jayabharat, K., Ashafaq, M, Venugopal, P., Achar, D.R.G. (2007). Investigation on the continuous drive friction welding of sintered powder metallurgical (P/M) steel and wrought copper parts, *Materials Science and Engineering A,* 454-455, pp. 114-123.

Jenkins, I. & Wood, J.V. (1991). Powder Metallurgy: An Overview. T*he Institute of Metals*, London, UK.

Juang, S.C. & Tarng, Y.S. (2002). Process Parameter Selection for Optmizing the Weld Pool Geometry in the Tig Welding of Stainless Steel, *Journal of Materials Processing Technology*, Vol. 22, No 1, pp. 33-37.

Kumar, T.S., Balusubramanian, V. & Sanavullah, M.Y. (2007). Influences of Pulsed Current Tungsten Inert Gas welding parameters on the Tensile properties of AA6061 Aluminum Alloy, *Materials Design*, 28, pp. 2080-2092.

Kurt, A.H., Ates, A., Durgutlu, A. & Karacif, K. (2004). Pexploring the Weldability of Powder Metal Parts, *Welding Journal*, 83 (12), pp. 34-37.

Lancaster, J.F. (1987). *Metallurgy of Welding*, London, UK.

Lenel, F.V. (1980). Powder Metallurgy: Principles and Applications, *Metal Powder Industries Federation*, New Jersey, USA

Lippold, J.C & Kotecki, D.J. (2005). *Welding Metallurgy and Weldability of Stainless Steels*, 5 ed., USA.

Metal Powder Industries Federation (2004). In : *Design Solutions Manual*, MPIF, New Jersey, USA

Pawan, K., Kolhe, K.P., Morey, S.J. & Datta, C.K. (2011). Process Parameters Optimization of an Aluminum Alloy with Pulsed Gas Tungsten Arc Welding (GTAW) Using Gas Mixtures, *Materials Science and Applications*, N.2, pp. 251-257.

Schatt, W. & Wieters, K-P. (1997). Powder Metallurgy: Processing and Materials, *European Powder Metallurgy Association*, Shrewbury.

Sudhakar, K.V., Sampathkumaran, P & Dwarakadasa, E.S. (2000). Dry Slinding wear in high density Fe-2% Ni based P/M alloys, *Wear,* 242, pp. 207-212

Suutala, N. (1983). Effect of solidification conditions on the solidification mode in austenitic stainless steels, *Metallurgical Transactions*, vol. 14, n. 2, pp. 191-197.

Thummler, F. & Oberacker, R. (1993). I*nstitute of Materials*, London, UK.

Wang, S.H., Chiu, P.K., Yang, J.R. & Fand, J. (2006). Gama (γ) phase transformation in Pulsed GTAW weld metal of Duplex Stainless Steel, *EurMaterials Science and Engineering A*, N. 420, pp. 26-33.

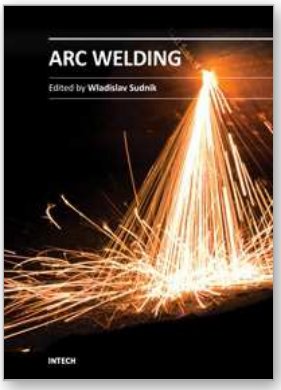

Arc Welding

Edited by Prof. Wladislav Sudnik

ISBN 978-953-307-642-3
Hard cover, 320 pages
Publisher InTech
Published online 16, December, 2011
Published in print edition December, 2011

Ever since the invention of arc technology in 1870s and its early use for welding lead during the manufacture of lead-acid batteries, advances in arc welding throughout the twentieth and twenty-first centuries have seen this form of processing applied to a range of industries and progress to become one of the most effective techniques in metals and alloys joining. The objective of this book is to introduce relatively established methodologies and techniques which have been studied, developed and applied in industries or researches. State-of-the-art development aimed at improving technologies will be presented covering topics such as weldability, technology, automation, modelling, and measurement. This book also seeks to provide effective solutions to various applications for engineers and researchers who are interested in arc material processing. This book is divided into 4 independent sections corresponding to recent advances in this field.

INTECH
open science | open minds

InTech Europe
University Campus STeP Ri
Slavka Krautzeka 83/A
51000 Rijeka, Croatia
Phone: +385 (51) 770 447
Fax: +385 (51) 686 166
www.intechopen.com

InTech China
Unit 405, Office Block, Hotel Equatorial Shanghai
No.65, Yan An Road (West), Shanghai, 200040, China
中国上海市延安西路65号上海国际贵都大饭店办公楼405单元
Phone: +86-21-62489820
Fax: +86-21-62489821